Stress-strain relationship of PDMS micropillar for force measurement application

Shazlina Johari[1,*] and *L. Y.* Shyan

[1]School of Microelectronic Engineering, Universiti Malaysia Perlis, Pauh Putra Kampus, 02610 Arau, Perlis, Malaysia

Abstract. There is an increasing interest to use polydimethylsiloxane (PDMS) based materials as bio-transducers for force measurements in the order of micro to nano Newton. The accuracy of these devices relies on appropriate material characterization of PDMS and modelling to convert the micropillar deformations into the corresponding forces. Previously, we have reported on fabricated PDMS micropillar that acts as a cylindrical cantilever and was experimentally used to measure the force of the nematode *C. elegans*. In this research, similar PDMS micropillars are designed and simulated using ANSYS software. The simulation involves investigating two main factors that is expected to affect the force measurement performance; pillar height and diameter. Results show that the deformation increases when pillar height is increased and the deformation is inversely proportional to the pillar diameter. The maximum deformation obtained is 713 um with pillar diameter of 20 um and pillar height of 100 um. Results of stress and strain show similar pattern, where their values decreases as pillar diameter and height is increased. The simulated results are also compared with the calculated displacement. The trend for both calculated and simulated values are similar with 13% average difference.

1 Introduction

C. elegans is a non-parasitic worm that has been extensively utilized for genetic model purposes to explore the correlation concerning genes and movement at the neuronal level. The reason for this is predominantly due to its transparency, having a nervous system so simple with merely 302 neurons, and a completely sequenced genome. The understanding of the nervous system, which coordinates the movements/actions and transmits signal between different body parts can potentially help to discover basic mechanism behind the actions of organism. In order to study *C. elegans* propulsion, research has been conducted to measure the worm's movement force which is induced by the contraction of their body wall muscle. The relationship between the nerves and the muscles in charge for the force generation in the neuromuscular system during the worm's motion can be obtained. Information regarding the locomotion forces can also be beneficial for the progress of therapy for muscle disorders, neurodegenerative [1] and humans genetic disease such as muscular dystrophy [2-4]. As the worm is small with the length of approximately 1 mm and the estimated width of 100µm, the existing sensors used in millimeter and larger scales are not capable of sensing the forces at the micro-Newton level.

Polydimethylsiloxane (PDMS) is a silicon based material consisting of a base part and a curing agent. The viscous polymer liquid changes into a solid elastic structure when both components are mixed and cured at a certain temperature. The use of PDMS pillar as force sensing mechanism have been applied in preceding works, as summarized in Table 1. The force obtained is based on the dimension of pillar used.

Table 1. PDMS micropillars as force sensor

Target	Pillar Dimension	Force applied
Mouse oocyte [5] (D: 75 um)	H: 45 um D: 12 um	50 nN - 550 nN
Cardiac myocyte [6] (H: 100-150 um D: 15-20 um)	H: 8 um D: 2 um	47.9 nN - 175 nN
D. melanogaster larvae [7] (H: 1000-1300 um D: 450-550 um)	H: 153 um D: 50 um	~ 32.61 ± 8.68 µN

Previously, the application of PDMS micropillars as a force sensor to measure *C. elegans* locomotion has been demonstrated [8], where the measurement of the worm locomotion forces were conducted experimentally. The microfabricated device consists of several parallel rows of vertical cantilever-like micropillars supported by the channel base. Each pillar functions as an independent force-measuring unit dedicated to one individual *C. elegans*. The worm locomotion force was measured experimentally with force resolution of 3.13 µN for worm body width of 100 µm. Since the nematode body sizes ranges according to their developmental stages [9],

* Corresponding author: shazlinajohari@unimap.edu.my

it is essential to predict the worm locomotion forces based on their body width.

In this work, PDMS micropillars with various dimension are designed and simulated. From the simulation conducted, the force measurement of worm locomotion could be predicted from the displacement obtained by applying reasonable range of input forces. The distributed force was represented by an equivalent point load on the pillar. This load results in an equivalent deflection of the pillar tip [10]. Deflection of a cantilever beam is attributed to both bending and shear incurred by the equivalent force load. When the aspect ratio (i.e. height-to-diameter ratio) of a cantilever beam is greater than 5, deflection due to the shear can be safely ignored as it contributes less than 5% to the total deflection [11]. However, as the aspect ratio of the micropillar is smaller than 5, hence both bending and shear must be considered in the force-deflection mechanics model. The equivalent displacement of the micropillar is calculated using Equation (1),

$$\Delta = \left\{ \left(\frac{l^3}{3EI} + \frac{d^2(1+\gamma)l}{4EI} \right) + \frac{l^2}{2EI}(h-l) \right\} f \qquad (1)$$

where f is the force applied, Δ is the displacement, I is the area moment of inertia, γ is the Poisson's ratio for PDMS, l, d and h are pillar length, diameter and height respectively, and E is the PDMS Young's Modulus.

2 Design and Simulation

The design of the micropillar is based on a cylindrical cantilever as shown in Figure 1. The pillar height, h and diameter, d is varied and their effect on the displacement, stress and strain was studied. The material properties used during the simulation are indicated in Table 1. Based on previous research, [8], the force exerted by the *C. elegans* is in the range from 5 - 70 µN. Thus, the forces used in ANSYS simulation are selected to be 5, 10, 20, 40, 60 and 80 µN. The deformation of the micropillar is observed and recorded. The force applied is set as a nodal or point force being exerted from the side of the micropillar, similar to their natural locomotion, where the worm moves by pushing their body and exerting force against their surroundings.

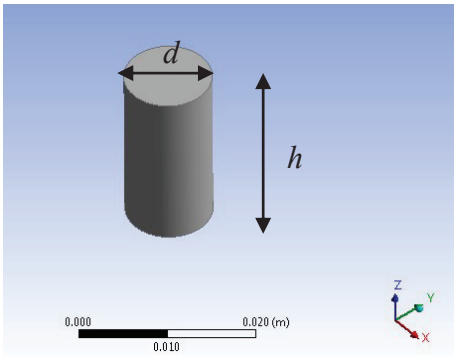

Fig. 1. Micropillar design with diameter, d and height, h

Table 2. PDMS Material Properties

Parameter	Value
Young's Modulus	1.47 MPa
Poisson's Ratio	0.48
Bulk Modulus	12.25 MPa
Shear Modulus	0.497 MPa

3 Results and Discussion

There are three output obtained from simulation, namely the deformation of the micropillar at a certain force input, stress distributed along the pillar height and the strain produced on the pillar during deformation.

(a)

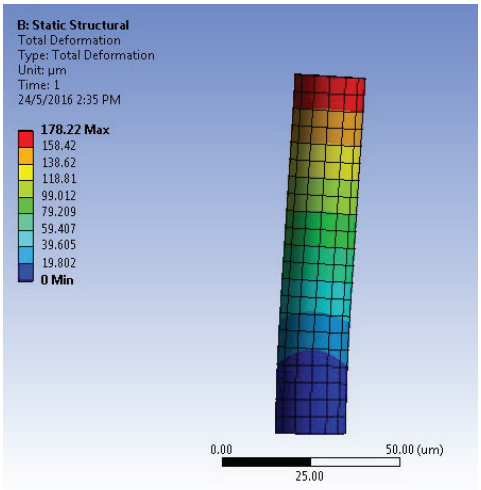

(b)

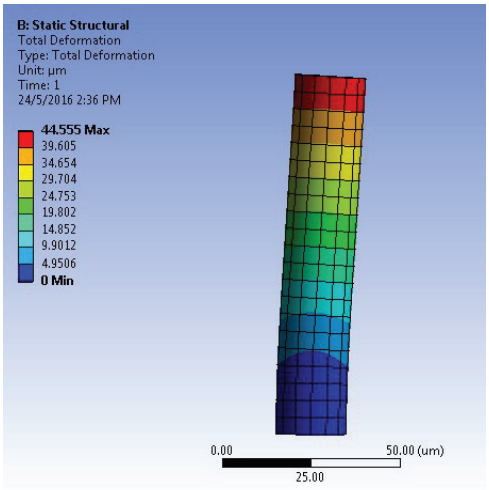

(c)

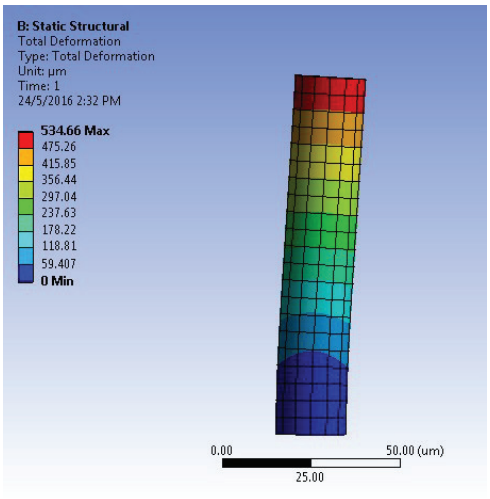

Fig. 2. Total deformation generated by ANSYS at diameter 20 µm when applying different forces. (a) 5µN (b) 20µN (c) 60µN

When point load are applied to the microcantilever, it will cause different stress levels generated on the microcantilever, thus, resulting in the displacement of the microcantilever. Fig. 2 shows the deformation results for pillar diameter of 20 µm and pillar height of 100 µm with applied force of 5, 20 and 60 µN. The highest displacement can be seen at the free end of the microcantilever while the maximum stress point is located at the fixed end of the microcantilever. It can be observed that the deformation occurs at the same place which is at the edge of the free end of the pillar. However, the maximum deformation of each force applied is different, which are 44.555 µm, 178.22 µm, and 534.66 µm for force of 5 µN, 20 and 60 µN respectively. The blue colour indicates the smallest deformation, since the part is the fixed support, where the fixed position is held in position. The changes of colour indicated different level of deformation of a micropillar. Each colour indicates different bending level of the micropillar.

During the simulation, the pillar diameter are varied while the pillar height is fixed to 100 um in order to see the effects of the micropillar dimension on the deformation, as shown in Fig. 3. For each pillar diameter, the simulated displacement show similar increasing trend as the force is increasingly applied. When pillar diameter is increased from 40 um to 60 um, the displacement roughly decrease 74%. When pillar diameter is bigger, the pillar aspect ratio will decrease, hence will result in the decrease of the pillar displacement. For pillar diameter of 40 um, the highest displacement is recorded at 49 um with applied force of 80 uN. The minimum recorded displacement is 125 nm when the pillar diameter is set to 120 um subjected to 100 um pillar height.

Next, the pillar diameter is fixed at 50 um while its height were varied from 80 um to 200 um. Fig. 4 depicts the variation in the micropillar displacement with respect to varying input force ranging from minimum of 5uN to maximum of 80 uN. The maximum deformation obtained at the applied input force of 80 µN is 18.201 µm when pillar height is 80 µm. The displacement value

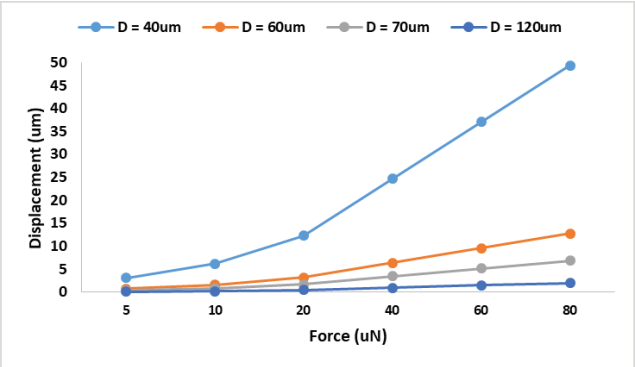

Fig. 3. Graph of displacement versus force for varying pillar diameter

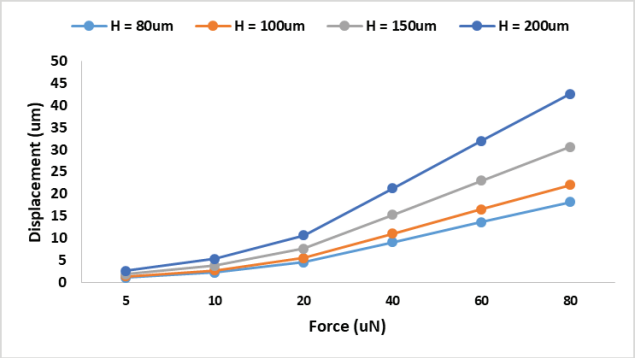

Fig. 4. Graph of displacement versus force for varying pillar height

increases 17.44% to 22.05 µm when pillar height is increased by 20 um. Then, this value increase 28.06% to 30.65 µm for pillar height of 150 µm and continue to increase by 28.03% to 42.6 µm at pillar height of 200 µm. The deviation in the displacement obtained is relatively smaller when compared to the displacement results from changes made in pillar diameter. A change of 100 µm (from 200 µm to 300 µm) only showed a deformation different of 13.033 µm (different of deformation at height 200 µm and 300 µm), which is increasing by 23.43%. The range of deflection obtained for varying pillar height and pillar diameter is similar, which is from 100 nm to 40 um. This shows that the aspect ratio critically influence the pillar bending performance.

We also measured the stress-strain relationship of the PDMS micropillar based on varying pillar height and diameter. At pillar diameter of 20 µm and fixed pillar height of 100 µm, the simulated stresses are 0.31 MPa, 0.62 MPa, 1.24 MPa, 2.47 MPa, 3.71 MPa and 4.94 MPa when force applied is 5 to 80 uN. Since stress is related to the force applied against a certain surface area, the stress value is increasing when the applied force is also increased. The effect of the pillar diameter on the stress distribution shows that as the pillar diameter increases, stress required to bend the pillar also increases. The changes in height showed opposite result as when the diameter is varied, where the stress distributed decreased when pillar height is increased.

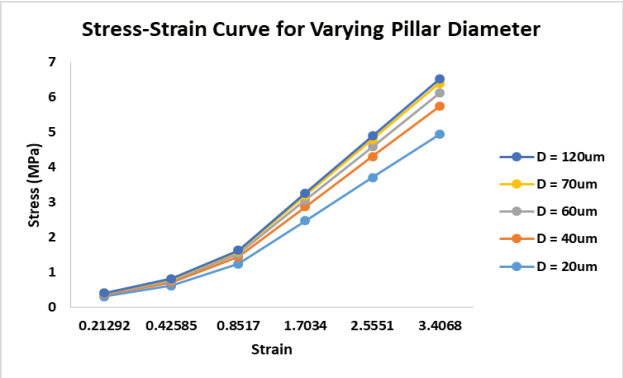

Fig. 5. Stress-strain curve of micropillar force for varying pillar diameter

The pillar with 50 µm diameter and 80 µm height shows a large stress deviation, which is 0.055 MPa, 0.11 MPa, 0.22 MPa, 0.44 MPa, 0.66 MPa and 0.87 MPa for applied force of 5 µN, 10 µN, 20 µN, 40 µN, 60 µN and 80 µN respectively. These simulated stresses are much different then 100 µm height, increasing height by 20 um only showed 0.029 MPa, 0.057 MPa, 0.113 MPa, 0.23 MPa, 0.34 MPa and 0.46 MPa for applied force of 5 µN, 10 µN, 20 µN, 40 µN, 60 µN and 80 µN correspondingly. In essence, materials experience strain when they are subject to stress. The relationship between stress and strain is different for different materials, and can be depicted by plotting stress against strain. The stress-strain curve that we obtained is comparable with existing work that reported on the stress-strain relationship of PDMS [12]. It is also important to note that the stress-strain curve is highly influenced by the PDMS material properties, hence resulting in a non-linear curve. Since this work is purely simulation, the material properties have been predefined prior to simulation, as shown in Table1.

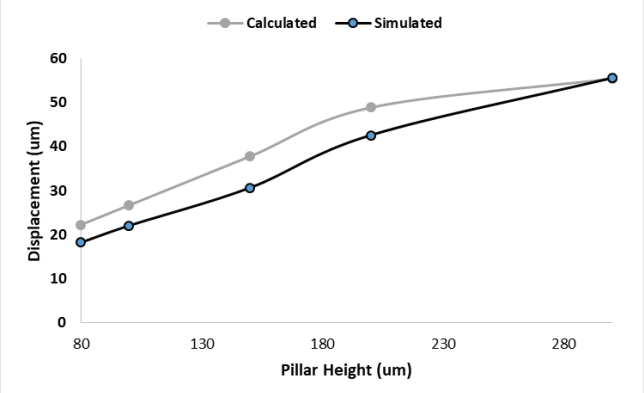

Fig. 6. Calculated and simulated value of pillar displacement for varying pillar height

The simulated results are also compared with the calculated displacement using Equation 1. The simulated and calculated value of displacement for constant input force of 80 µN are plotted in Fig. 6. For example, for pillar height of 80 µm, the calculated displacement is 22.2 µm compared to 18.2 µm simulated value. As the pillar height is increased, the trend for both calculated and simulated values are similar with 13% average difference. When pillar height is 300 µm, both calculated and simulated displacement value is 55 µm. This shows that the conducted simulation of this work is in agreement with the theoretical calculated displacement.

4 Conclusion

The high elastic property of PDMS allows this material to be widely used as force measurement apparatus of biological organism. We have design and investigated the bending behaviour of micropillar with varying height and diameter by observing its displacement. We found that pillar aspect ratio influence the output displacement the most, where for pillar diameter of 20 µm and pillar height of 100 µm, the maximum displacement is obtained. In terms of stress-strained curve, the result is comparable with preceding works reported. The simulated results are also compared with the calculated displacement using bending equation and both simulated and calculated value depict similar increasing trends.

We are grateful for the funding provided by FRGS 9003:00405 and the authors would like to thank School of Microelectronic (SoME), Universiti Malaysia Perlis for their technical assistance and supports.

References

1. M. Dimitriadi, J. N. Sleigh, A. Walker, H. C. Chang, A. Sen, G. Kalloo, J. Harris, T. Barsby, M. B. Walsh, J. S. Satterlee, C. Li, D. Van Vactor, S. Artavanis-Tsakonas, and A. C. Hart, PLoS Genetic, **6**, p. e1001172 (2010)
2. C. I. Bargmann, Science, vol. 282, pp. 2028-33 (1998)
3. J. E. Mendel, H. C. Korswagen, K. S. Liu, Y. M. Hajdu-Cronin, M. I. Simon, R. H. Plasterk, and P. W. Sternberg, Science, **267**, pp. 1652-5 (1995)
4. L. S. Nelson, M. L. Rosoff, and C. Li, Science, vol. 281, pp. 1686-90 (1998)
5. X. Liu, J. Shi, Z. Zong, R. Fernandes, R. F. Casper, A. Jurisicova, K.T Wang and Y. Sun, *15th International Conference on Miniaturized Systems for Chemistry and Life Sciences* (2011)
6. Y. Zhao and X. Zhang, Sensors and Actuators A 125 398–404 (2006)
7. S.M. Khare1, V. Venkataraman1 and S.P. Koushika, *18th International Conference on Miniaturized Systems for Chemistry and Life Sciences* (2014)
8. S. Johari, V. Nock, M. M. Alkaisi, W Wang, Lab Chip, **13** (9), pp. 1699-1707 (2013)
9. S. E. Hulme, S. S. Shevkoplyas, A. P. McGuigan, J. Apfeld, W. Fontana, and G. M. Whitesides, Lab Chip, **10**, pp. 589-97 (2010)

10. A. C. Ugural and S. K. Fenster, Advanced Strength and Applied Elasticity (2003)
11. A. Ghanbari, V. Nock, S. Johari, R. J Blaikie, X. Q. Chen, W. Wang, Journal of Micromechanics and Microengineering 22(9): 095009 (2012)
12. K. Khanafer, A. Duprey, M. Schlicht and R. Berguer, Biomed Microdevices 11:503–508 (2009)